A gravitational-wave standard siren measurement of the Hubble constant

B. Abbott[1], M. Others[2] & E. M. Partners[3]

[1] *LIGO*

[2] *Virgo*

[3] *Everywhere*

P1700296-v3

September 29, 2017

We report the first determination of the Hubble constant, which is the local expansion rate of the Universe, using gravitational wave measurements. The spiraling together of two compact objects, such as neutron stars or black holes, is a "standard siren": the waves emitted tell us the distance to the binary. The observation by the LIGO and Virgo detectors of the neutron-star merger event GW170817, combined with follow-up optical observations of the post-merger explosion, allows us to measure both the distance and the recession velocity of the standard siren's host galaxy, NGC 4993, and thereby infer the Hubble constant. Our measured value is consistent with existing estimates, while being completely independent of them. Future gravitational wave observations of merger events will enable more precise measurements of the Hubble constant.

The detection of GW170817[1] heralds the age of multi-messenger astronomy, with the observations of gravitational-wave (GW) and electromagnetic (EM) emission from the same transient source. On 17 August 2017 the network of Advanced Laser Interferometer Gravitational-wave Observatory (LIGO)[2] and Virgo[3] detectors observed GW170817, a strong signal from the merger of a compact-object binary. The source was localized to a region of 28 deg^2 (90% credible region). Independently, the *Fermi* Gamma-Ray Burst Monitor (GBM)[4] detected a weak Gamma Ray Burst (GRB) event GRB170817A consistent with the same sky region, less than 2 seconds after the compact binary merger[5–7]. The LIGO-Virgo localization region was subsequently observed by a number of optical astronomy facilities[8], resulting in the identification of an optical transient signal within ~ 10 arcsec of the galaxy NGC 4993 (Swope, DECam, DLT40 2017 in prep., Valenti et al. ApJL, accepted, LCOGT, VISTA, MASTER). GW170817 is therefore the first source to have been detected in both GWs and EM waves, and the first GW source with a known host galaxy. This event can therefore be used as a *standard siren*[9–13] to determine the Hubble constant, combining the distance inferred purely from the GW signal with the Hubble flow velocity of the galaxy containing the electromagnetic transient. Such measurements do not require any form of cosmic "distance ladder"[14]; the GW analysis directly estimates the luminosity distance out to cosmological scales.

The Hubble constant H_0 measures the mean expansion rate of the Universe. At nearby distances ($d \lesssim 100\,\mathrm{Mpc}$) it is well approximated by the expression

$$v_H = H_0 d, \tag{1}$$

where v_H is the local "Hubble flow" velocity of a source, and d is the distance to the source. At this nearby distance all cosmological distance measures (such as luminosity distance and comoving distance) differ by less than 1%, so we do not distinguish among them. We are similarly insensitive to the values of other cosmological parameters, such as Ω_m and Ω_Λ. An analysis of the GW data finds that GW170817 occurred at a distance $d = 43.8^{+2.9}_{-6.9}$ Mpc[1]. (All values are quoted as the maximum posterior value with the minimal width 68.3% credible interval). To obtain the Hubble flow velocity at the position of GW170817, we use the optical identification of the host galaxy NGC 4993[8]. This identification is based solely on the 2-dimensional projected offset and is independent of any assumed value of H_0. The position and redshift of this galaxy allow us to estimate the appropriate value of the Hubble flow velocity.

The original standard siren proposal[9] did not rely on the unique identification of a host galaxy. As long as a possible set of host galaxies can be identified for each GW detection, by combining information from ~ 100 independent detections, an estimate of H_0 with $\sim 5\%$ uncertainty can be obtained event without the detection of any transient optical counterparts[15]. If an EM counterpart has been identified but the host galaxy is unknown, the same statistical method can be applied but using only those galaxies in a narrow beam around the location of the optical counterpart. However, such statistical analyses are sensitive to a number of complicating effects, including the incompleteness of current galaxy catalogs[16] or the need for dedicated follow-up surveys, as well as a range of selection effects[17]. In what follows we exploit the identification of NGC 4993 as the host galaxy of GW170817 to perform a standard siren measurement of the Hubble constant[10–13].

The gravitational wave observation

Analysis of the GW data associated with GW170817 produces estimates for the parameters of the

[1]The distance quoted here differs from that in other studies[1], since here we assume that the optical counterpart represents the true sky position of the GW source instead of marginalizing over a range of potential sky positions.

source, under the assumption that General Relativity is the correct model of gravity. Parameters are inferred within a Bayesian framework[18] by comparing strain measurements[1] in the two LIGO detectors and the Virgo detector with the gravitational waveforms expected from the inspiral of two point masses[19] under general relativity. We are most interested in the joint posterior distribution on the luminosity distance and binary orbital inclination angle. For the analysis in this paper we fix the location of the GW source on the sky to the identified location of the counterpart[20]. This analysis uses algorithms for removing short-lived detector noise artifacts[1,21] and employs approximate point-particle waveform models[19,22,23]. We have verified that the systematic changes in the results presented here from incorporating non-point-mass (tidal) effects[24,25] and from different data processing methods are much smaller than the statistical uncertainties in the measurement of H_0 and the binary orbital inclination angle.

The distance to GW170817 is estimated from the GW data alone to be $43.8^{+2.9}_{-6.9}\,\mathrm{Mpc}$. The $\sim 15\%$ uncertainty is due to a combination of statistical measurement error from the noise in the detectors, instrumental calibration uncertainties[1], and a geometrical factor dependent upon the correlation of distance with inclination angle. The GW measurement is consistent with the distance to NGC 4993 measured using the Tully-Fisher relation, $d_{\mathrm{TF}} = 41.1 \pm 5.8\,\mathrm{Mpc}$[14,26].

The measurement of the GW polarization is crucial for inferring the binary inclination. This inclination, ι, is defined as the angle between the line of sight vector from the source to the detector and the angular momentum vector of the binary system. Observable electromagnetic phenomena cannot typically distinguish between face-on and face-off sources, and therefore are usually characterized by a viewing angle: $\min(\iota, 180\,\mathrm{deg} - \iota)$. By contrast, GW measurements can identify whether a source is rotating counter-clockwise or clockwise with respect to the line of sight, and thus ι ranges from 0 to $180\,\mathrm{deg}$. Previous GW detections by LIGO had large uncertainties in luminosity distance and inclination[27] because the two LIGO detectors that were involved are nearly co-aligned, preventing a precise polarization measurement. In the present case, thanks to Virgo as an additional detector, the cosine of the inclination can be constrained at 68.3% (1-σ) confidence to the range $[-1, -0.81]$ corresponding to inclination angles between $[144, 180]\,\mathrm{deg}$. This implies that the plane of the binary orbit is almost, but not quite, perpendicular to our line of sight to the source ($\iota \approx 180\,\mathrm{deg}$), which is consistent with the observation of a coincident GRB[5–7] (LVC, GBM, INTEGRAL 2017 in prep., Goldstein et al. 2017, ApJL, submitted, and Savchenko et al. 2017, ApJL, submitted).

The electromagnetic observations

EM follow-up of the GW sky localization region[8] discovered an optical transient[20,28–31] in close proximity to the galaxy NGC 4993. The location of the transient was previously observed by the *Hubble Space Telescope* on 2017 April 28 UT and no sources were found within 2.2 arcseconds down to 25.9 mag[32]. We estimate the probability of a random chance association between the optical counterpart and NGC 4993 to be 0.004% (see the methods section for details). In what follows we assume that the optical counterpart is associated with GW170817, and that this source resides in NGC 4993.

To compute H_0 we need to estimate the background Hubble flow velocity at the position of NGC 4993. In the traditional electromagnetic calibration of the cosmic "distance ladder"[14], this step is commonly carried out using secondary distance indicator information, such as the Tully-Fisher relation[26], which allows one to infer the background Hubble flow velocity in the local Universe scaled back from more distant secondary indicators calibrated in quiet Hubble flow. We do not adopt this approach here, however, in order to preserve more fully the independence of our results from the electromagnetic distance ladder. Instead we estimate the Hubble flow velocity at the position of NGC 4993 by correcting for local peculiar motions.

NGC 4993 is part of a collection of galaxies, ESO-508, whose center-of-mass recession velocity relative to our local CMB frame[33] is[34,35] $3327 \pm 72\,\mathrm{km\,s^{-1}}$. We correct the group velocity by $310\,\mathrm{km\,s^{-1}}$ due to the coherent bulk flow[36,37] towards The Great Attractor (see Methods section for details). The standard error on our estimate of the peculiar velocity is $69\,\mathrm{km\,s^{-1}}$, but recognizing that this value may be sensitive to details of the bulk flow motion that have been imperfectly modelled, in our subsequent analysis we adopt a more conservative estimate[37] of $150\mathrm{km\,s^{-1}}$ for the uncertainty on the peculiar velocity at the location of NGC 4993, and fold this into our estimate of the uncertainty on v_H. From this, we obtain a Hubble velocity $v_H = 3024 \pm 166\,\mathrm{km\,s^{-1}}$.

Analysis

Once the distance and Hubble velocity distributions have been determined from the GW and EM data, respectively, we can constrain the value of the Hubble constant. The measurement of the distance is strongly correlated with the measurement of the inclination of the orbital plane of the binary. The analysis of the GW data also depends on other parameters describing the source, such as the masses of the components[18]. Here we treat the uncertainty in these other variables by marginalizing over the posterior distribution on system parameters[1], with the exception of the position of the system on the sky which is taken to be fixed at the location of the optical counterpart.

We carry out a Bayesian analysis to infer a posterior distribution on H_0 and inclination, marginalized over uncertainties in the recessional and peculiar velocities; see the Methods section for details. Figure 1 shows the marginal posterior for H_0. The maximum a posteriori value with the minimal 68.3% credible interval is $H_0 = 70^{+12}_{-8}\,\mathrm{km\,s^{-1}\,Mpc^{-1}}$. Our estimate agrees well with state-of-the-art determinations of this quantity, including CMB measurements from Planck[38] ($67.74 \pm 0.46\,\mathrm{km\,s^{-1}\,Mpc^{-1}}$, "TT,TE,EE+lowP+lensing+ext") and Type Ia supernova measurements from SHoES[39] ($73.24 \pm 1.74\,\mathrm{km\,s^{-1}\,Mpc^{-1}}$), as well as baryon acoustic oscillations measurements from SDSS[40], strong lensing measurements from H0LiCOW[41], high-l CMB measurements from SPT[42], and Cepheid measurements from the HST key project[14]. Our measurement is a new and independent determination of this quantity. The close agreement indicates that, although each method may be affected by different systematic uncertainties, we see no evidence at present for a systematic difference between GW and EM-based estimates. As has been much remarked upon, the Planck and SHoES results are inconsistent at $\gtrsim 3\sigma$ level. Our measurement does not resolve this tension, falling neatly between the two values and being broadly consistent with both.

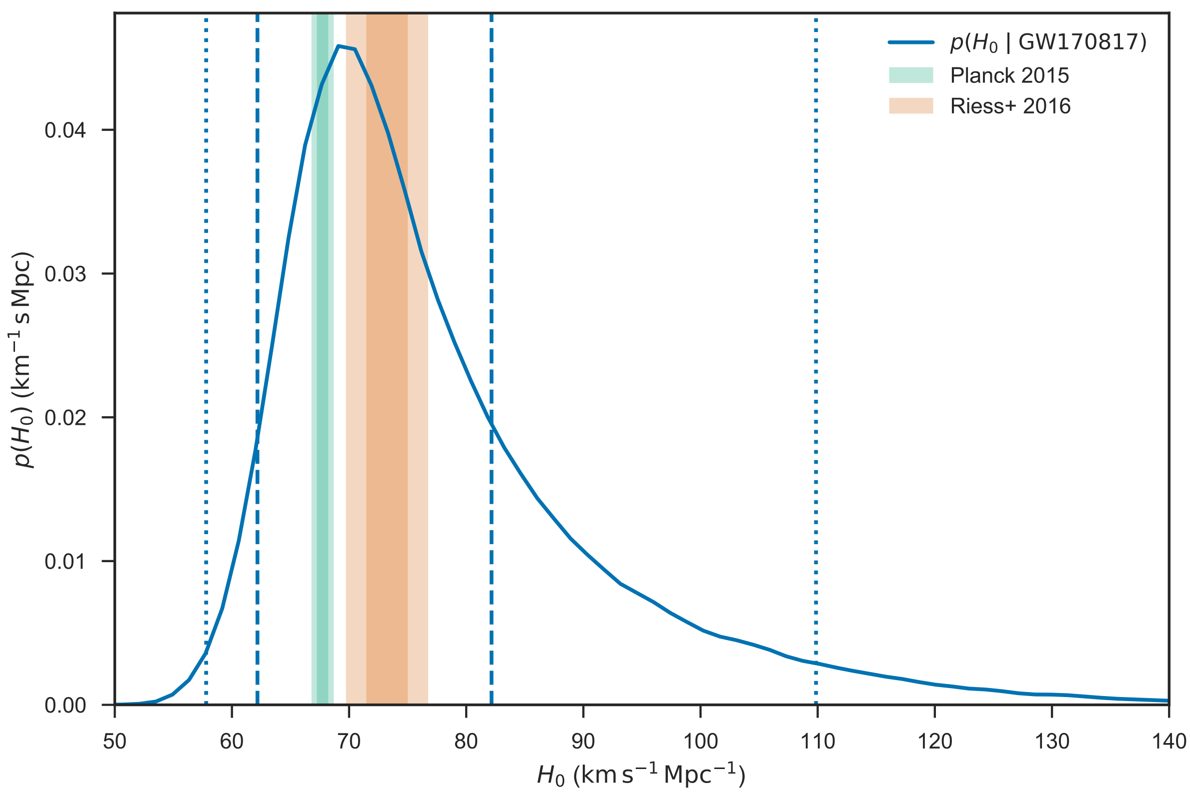

Figure 1 GW170817 measurement of H_0 . Marginalized posterior density for H_0 (blue curve). Constraints at 1- and 2-σ from Planck[38] and SHoES[39] are shown in green and orange. The maximum a posteriori and minimal 68.3% credible interval from this PDF is $H_0 = 70^{+12}_{-8}\,\mathrm{km\,s^{-1}\,Mpc^{-1}}$. The 68.3% (1$\sigma$) and 95.4% (2$\sigma$) minimal credible intervals are indicated by dashed and dotted lines.

One of the main sources of uncertainty in our measurement of H_0 is due to the degeneracy between distance and inclination in the GW measurements. A face-on binary far away has a similar amplitude to an edge-on binary closer in. This relationship is captured in Figure 2, which shows posterior contours in the H_0–ι parameter space.

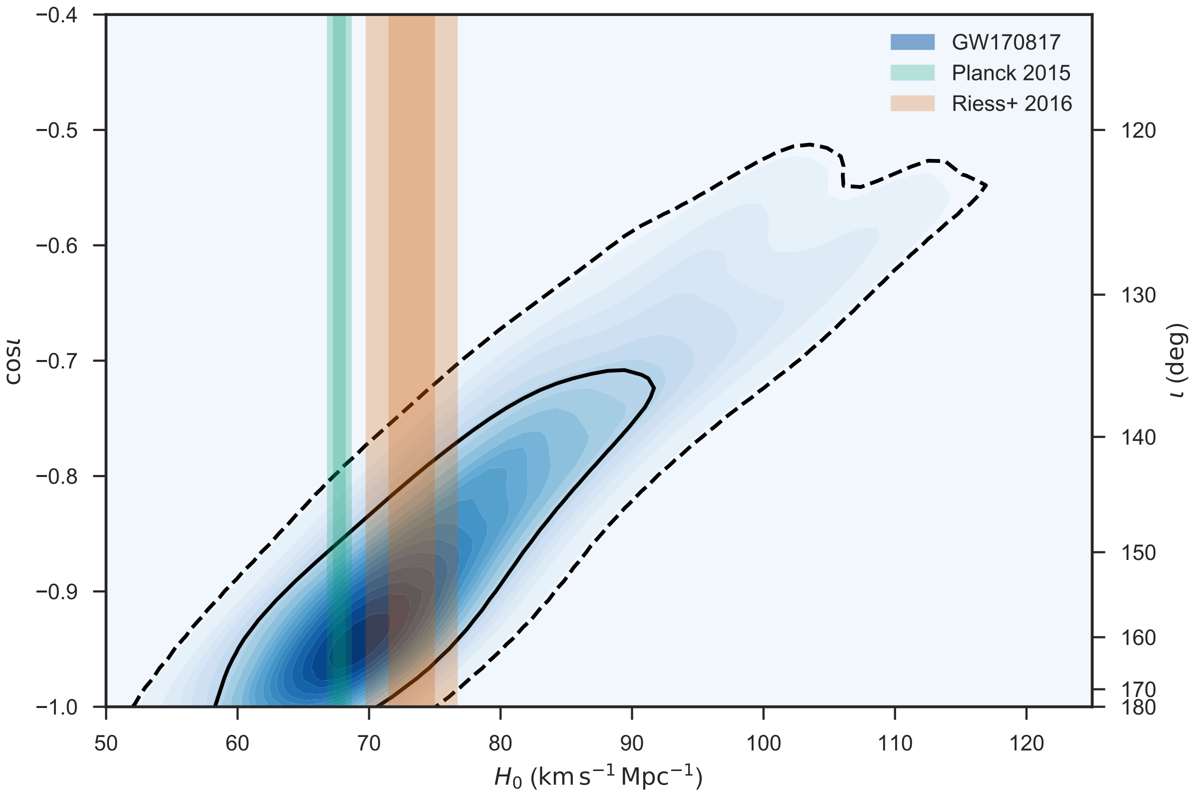

Figure 2 Inference on H_0 and inclination. Posterior density of H_0 and $\cos\iota$ from the joint GW-EM analysis (blue contours). Shading levels are drawn at every 5% credible level, with the 68.3% (1σ, solid) and 95.4% (2σ, dashed) contours in black. Values of H_0 and 1- and 2-σ error bands are also displayed from Planck[38] and SHoES[39]. As noted in the text, inclination angles near $180\,\mathrm{deg}$ ($\cos\iota = -1$) indicate that the orbital angular momentum is anti-parallel with the direction from the source to the detector.

The posterior in Figure 1 results from the vertical projection of Figure 2, marginalizing out uncertainties in the cosine of inclination to derive constraints on the Hubble constant. Alternatively, it is possible to project horizontally, and thereby marginalize out the Hubble constant to derive constraints on the cosine of inclination. If instead of deriving H_0 independently we take the existing constraints on H_0[38,39] as priors, we are able to significantly improve our constraints on $\cos\iota$ as shown in Figure 3. Assuming the Planck value for H_0, the minimal 68.3% credible interval for the cosine of inclination is $[-1, -0.92]$ (corresponding to an inclination angle range $[157, 177]\,\mathrm{deg}$). For the SHoES value of H_0, it is $[-0.97, -0.85]$ (corresponding to an inclination angle range $[148, 166]\,\mathrm{deg}$). For this latter SHoES result we note that the face-off $\iota = 180\,\mathrm{deg}$ orientation is just outside the 90% confidence range. It will be particularly interesting to compare these constraints to those from modeling of the short GRB, afterglow, and optical counterpart associated with GW170817.

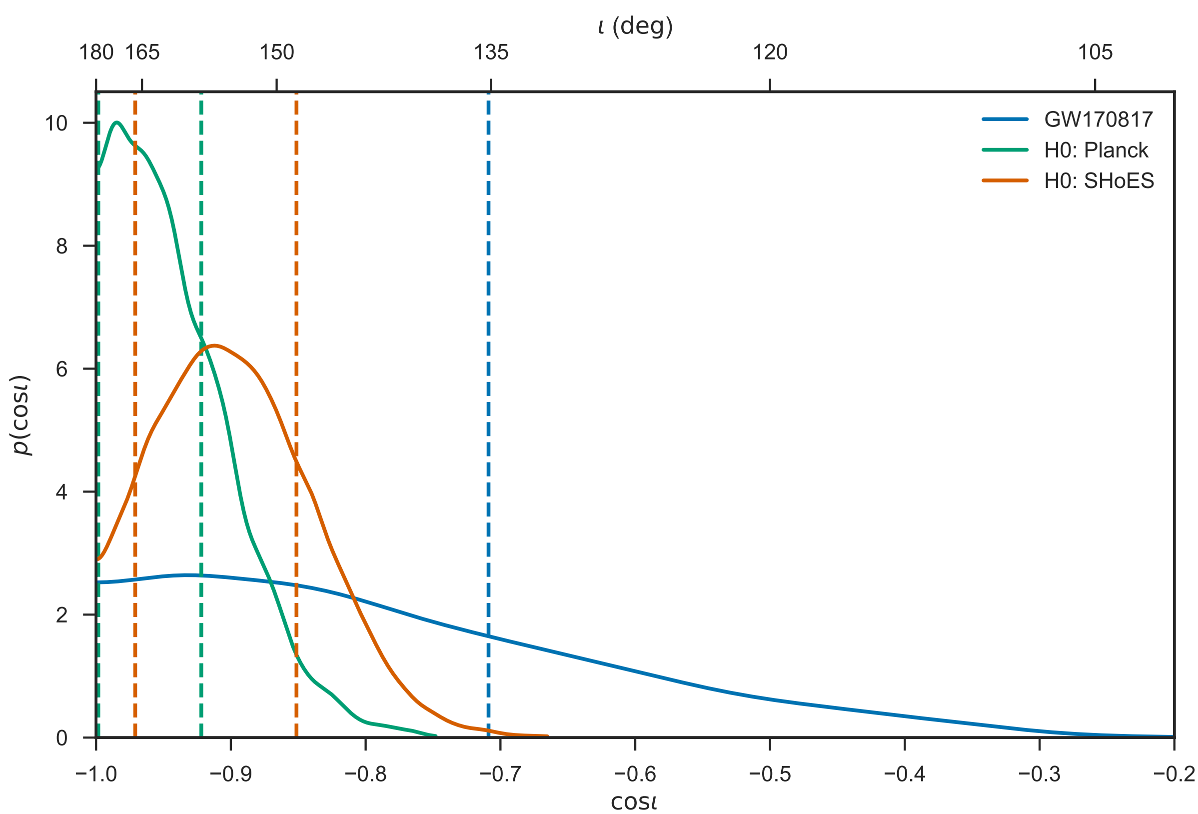

Figure 3 Constraints on the inclination. Posterior density on $\cos\iota$, for various as-

sumptions about the prior distribution of H_0. The analysis of the joint GW and EM data with a $1/H_0$ prior density gives the blue curve; using values of H_0 from Planck[38] and SHoES[39] as a prior on H_0 gives the green and red curves. Choosing a narrow prior on H_0 converts the precise Hubble velocity measurements for the group containing NGC 4993 to a precise distance measurement, breaking the distance inclination degeneracy, and leading to strong constraints on the inclination. Minimal 68.3% (1σ) credible intervals are indicated by dashed lines. Because our prior on inclination is flat on $\cos\iota$ the densities in this plot are proportional to the marginalised likelihood for $\cos\iota$.

Discussion

We have presented a standard siren determination of the Hubble constant, using a combination of a GW distance and an EM Hubble velocity estimate. Our measurement does not use a "distance ladder", and makes no prior assumptions about H_0. We find $H_0 = 70^{+12}_{-8}\,\mathrm{km\,s^{-1}\,Mpc^{-1}}$, which is consistent with existing measurements[38,39]. This first GW–EM multi-messenger event demonstrates the potential for cosmological inference from GW standard sirens. The coming years can be expected to bring additional multi-messenger binary neutron star events, as well as numerous detections of binary black hole mergers[43,44], for which EM counterparts are not expected. Combining subsequent independent measurements of H_0 from these future standard sirens will only improve the estimate made from GW170817, leading to an era of percent-level GW cosmology.

Methods

Probability of optical counterpart association with NGC 4993

We calculate the probability that an NGC 4993-like galaxy (or brighter) is misidentified as the host by asking how often the centre of one or more such galaxies falls by random chance within a given angular radius θ of the counterpart. Assuming Poisson counting statistics this probability is given by $P = 1 - \exp\left[-\pi\theta^2 S(< m)\right]$ where $S(< m)$ is the surface density of galaxies with apparent magnitude equal to or brighter than m. From the local galaxy sample distribution in the infrared (K-band) apparent magnitude[45] we obtain $S(< K) = 1.56 \exp\left(0.64(K - 10) - 0.7\right)\ \mathrm{deg}^{-2}$. As suggested by[46], we set θ equal to twice the half-light radius of the the galaxy for which we use the NGC 4993's diameter ~ 1.1 arcmin, as measured in the near infrared band (the predominant emission band for early-type galaxies). Using $K = 9.224$ mag taken from the 2MASS survey[47] for NGC 4993, we find the probability of random chance association is $P = 0.004\%$.

Finding the Hubble velocity of NGC 4993

In previous EM determinations of the cosmic "distance ladder", the Hubble flow velocity of the local calibrating galaxies has generally been estimated using redshift-independent secondary galaxy distance indicators, such as the Tully-Fisher relation or type Ia supernovae, calibrated with more distant samples that can be assumed to sit in quiet Hubble flow [14]. We do not adopt this approach for NGC 4993, however, in order that our inference of the Hubble constant is fully independent of the electromagnetic distance scale. Instead we estimate the Hubble flow velocity at the position of NGC 4993 by correcting its measured recessional velocity for local peculiar motions.

NGC 4993 resides in a group of galaxies whose center-of-mass recession velocity relative to the Cosmic Microwave Background (CMB) frame[33] is[34,35] $3327 \pm 72\,\mathrm{km\,s^{-1}}$. We assume that all of the galaxies in the group are at the same distance and therefore have the same Hubble flow velocity, which we assign to be the Hubble velocity of GW170817. This assumption is accurate to within 1% given that the radius of the group is ~ 0.4 Mpc. To calculate the Hubble flow velocity of the group, we correct its measured recessional velocity by the peculiar velocity caused by the local gravitational field. This is a significant correction; typical peculiar velocities are 300 km/s, equivalent to 10% of the total recessional velocity at a distance of 40 Mpc.

We employ the 6dF galaxy redshift survey peculiar velocity map[36,48], which used more than 8,000 Fundamental Plane galaxies to map the peculiar velocity field in the Southern hemisphere out to redshift $z \simeq 0.055$. We weight the peculiar velocity corrections from this catalogue with a Gaussian kernel centered on NGC 4993's sky position and with a width of $8h^{-1}\,\mathrm{Mpc}$[2], typical of the widths used in the catalogue itself. There are 10 galaxies in the 6dF peculiar velocity catalog within one kernel width of NGC 4993. In the CMB frame[33], the weighted radial component of the peculiar velocity and associated uncertainty is $\langle v_p \rangle = 310 \pm 69\,\mathrm{km\,s^{-1}}$.

We verified the robustness of this peculiar velocity correction by comparing it with the velocity field reconstructed from the 2MASS redshift survey[37,49]. This exploits the linear relationship between the peculiar velocity and mass density fields smoothed on scales larger than about $8h^{-1}$ Mpc, and the constant of proportionality can be determined by comparison with radial peculiar velocities of individual galaxies estimated from e.g. Tully-Fisher and Type Ia super-

[2]The kernel width is independent of H_0 and is equivalent to a width of $800\,\mathrm{km\,s^{-1}}$in velocity space.

novae distances. Using these reconstructed peculiar velocities, which have a larger associated uncertainty[37] of $150\,\mathrm{km\,s^{-1}}$, at the position of NGC 4993 we find a Hubble velocity in the CMB frame of $v_H = 3047\,\mathrm{km\,s^{-1}}$ – in excellent agreement with the result derived using 6dF. We adopt this larger uncertainty on the peculiar velocity correction in recognition that the peculiar velocity estimated from the 6dF data may represent an imperfect model of the true bulk flow at the location of NGC 4993. For our inference of the Hubble constant we therefore use a Hubble velocity $v_H = 3024 \pm 166\,\mathrm{km\,s^{-1}}$ with 68.3% uncertainty.

Finally, while we emphasise again the independence of our Hubble constant inference from the electromagnetic distance scale, we note the consistency of our GW distance estimate to NGC 4993 with the Tully-Fisher distance estimate derived by scaling back the Tully-Fisher relation calibrated with more distant galaxies in quiet Hubble flow[26]. This also strongly supports the robustness of our estimate for the Hubble velocity of NGC 4993.

Summary of the model

Given observed data from a set of GW detectors, x_{GW}, parameter estimation is used to generate a posterior on the parameters that determine the waveform of the GW signal[1,18]. From this we can obtain the parameter estimation likelihood of the observed GW data, marginalized over all parameters characterizing the GW signal except d and $\cos\iota$,

$$p(x_{\mathrm{GW}} \mid d, \cos\iota) = \int p(x_{\mathrm{GW}} \mid d, \cos\iota, \vec{\lambda})\, p(\vec{\lambda}) \mathrm{d}\vec{\lambda}, \tag{2}$$

The other waveform parameters are denoted by $\vec{\lambda}$, with $p(\vec{\lambda})$ denoting the corresponding prior.

Given perfect knowledge of the redshift of the GW source, z_0, this posterior distribution can be readily converted into a posterior on $\cos\iota$ and $H_0 = cz_0/d$,

$$p(H_0, \cos\iota | x_{\rm GW}) \propto (cz_0/H_0^2)\, p(x_{\rm GW} \mid d = cz_0/H_0, \cos\iota)\, p_d(cz_0/H_0)\, p_\iota(\cos\iota), \qquad (3)$$

where $p_d(d)$ and $p_\iota(\cos\iota)$ are the prior distributions on distance and inclination. For the Hubble velocity $v_H = 3024\,{\rm km\,s^{-1}}$, the maximum a posteriori distance from the GW measurement of $43.8\,{\rm Mpc}$ corresponds to $H_0 = 69.0\,{\rm km\,s^{-1}\,Mpc^{-1}}$, so this procedure would be expected to generate a posterior on H_0 that peaks close to that value.

While the above analysis is conceptually straightforward, it makes a number of over-simplified assumptions. The Hubble-flow redshift cannot be determined exactly, the redshift must be corrected for peculiar velocities, and the effective prior on H_0 from the usual $p_d(d) \propto d^2$ prior used in GW parameter estimation is $p(H_0) \propto 1/H_0^4$. In addition, the logic in this model is that a redshift has been obtained first and the distance is then measured using GWs. As GW detectors cannot be pointed, we cannot target particular galaxies or redshifts for GW sources. In practice, we wait for a GW event to trigger the analysis and this introduces potential selection effects which we must consider. We will see below that the simple analysis described above does give results that are consistent with a more careful analysis for this first detection. However, the simple analysis cannot be readily extended to include second and subsequent detections, so we now describe a more general framework that does not suffer from these limitations.

We suppose that we have observed a GW event, which generated data $x_{\rm GW}$ in our detectors, and that we have also measured a recessional velocity for the host, v_r, and the peculiar velocity field, $\langle v_p \rangle$, in the vicinity of the host. These observations are statistically independent and so the combined likelihood is

$$p(x_{\rm GW}, v_r, \langle v_p \rangle \mid d, \cos\iota, v_p, H_0) = p(x_{\rm GW} \mid d, \cos\iota)\, p(v_r \mid d, v_p, H_0)\, p(\langle v_p \rangle \mid v_p). \qquad (4)$$

The quantity $p(v_r \mid d, v_p, H_0)$ is the likelihood of the recessional velocity measurement, which we model as

$$p\left(v_r \mid d, v_p, H_0\right) = N\left[v_p + H_0 d, \sigma_{v_r}\right](v_r) \qquad (5)$$

where $N\left[\mu, \sigma\right](x)$ is the normal (Gaussian) probability density with mean μ and standard deviation σ evaluated at x. The measured recessional velocity, $v_r = 3327\,\mathrm{km\,s^{-1}}$, with uncertainty $\sigma_{v_r} = 72\,\mathrm{km\,s^{-1}}$, is the mean velocity and standard error for the members of the group hosting NGC 4993 taken from the two micron all sky survey (2MASS)[34,35], corrected to the CMB frame[33]. We take a similar Gaussian likelihood for the measured peculiar velocity, $\langle v_p \rangle = 310\,\mathrm{km\,s^{-1}}$, with uncertainty $\sigma_{v_p} = 150\,\mathrm{km\,s^{-1}}$:

$$p\left(\langle v_p \rangle \mid v_p\right) = N\left[v_p, \sigma_{v_p}\right]\left(\langle v_p \rangle\right). \qquad (6)$$

From the likelihood (4) we derive the posterior

$$p(H_0, d, \cos\iota, v_p \mid x_{\rm GW}, v_r, \langle v_p \rangle) \propto \frac{p(H_0)}{\mathcal{N}_{\rm s}(H_0)}\, p(x_{\rm GW} \mid d, \cos\iota)\, p(v_r \mid d, v_p, H_0) \times\ p(\langle v_p \rangle \mid v_p)\, p(d)\, p(v_p)\, p(\cos\iota), \qquad (7)$$

where $p(H_0)$, $p(d)$, $p(v_p)$ and $p(\cos\iota)$ are the parameter prior probabilities. Our standard analysis assumes a volumetric prior, $p\left(d\right) \propto d^2$, on the Hubble distance, but we explore sensitivity to this choice below. We take a flat-in-log prior on H_0, $p\left(H_0\right) \propto 1/H_0$, impose a flat (i.e. isotropic) prior on $\cos\iota$, and a flat prior on v_p for $v_p \in [-1000, 1000]\,\mathrm{km\,s^{-1}}$. These priors characterise our beliefs about the cosmological population of GW events and their hosts before we make any additional measurements or account for selection biases. The full statistical model is summarized graphically in Figure 1. This model with these priors is our canonical analysis.

In Eq. (7), the term $\mathcal{N}_{\rm s}(H_0)$ encodes selection effects [43,50,51]. These arise because of the finite sensitivity of our detectors. While all events in the Universe generate a response in the detector, we will only be able to identify and hence use signals that generate a response of sufficiently high amplitude. The decision about whether to include an event in the analysis is a property of the data only, in this case $x_{\rm GW}$, v_r, $\langle v_p \rangle$, but the fact that we condition our analysis on a signal being detected, i.e., the data exceeding these thresholds, means that the likelihood must be renormalized to become the likelihood for detected events. This is the role of

$$\mathcal{N}_{\rm s}(H_0) = \int_{\rm detectable} \Big[p(x_{\rm GW} \mid d, \cos\iota, \vec{\lambda})\, p(v_r \mid d, v_p, H_0) \times p(\langle v_p \rangle \mid v_p)\, p(\vec{\lambda})\, p(d)\, p(v_p)\, p(\cos\iota) \Big]\, {\rm d}\vec{\lambda}\, {\rm d}d\, {\rm d}v_p\, {\rm d}\cos\iota\, {\rm d}x_{\rm GW}\, {\rm d}v_r\, {\rm d}\langle v_p \rangle, \tag{8}$$

where the integral is over the full prior ranges of the parameters, $(d, v_p, \cos\iota, \vec{\lambda})$, and over data sets that would be selected for inclusion in the analysis, i.e., exceed the specified thresholds. If the integral was over all data sets it would evaluate to 1, but because the range is restricted there can be a non-trivial dependence on parameters characterizing the population of sources, in this case H_0.

In the current analysis, there are in principle selection effects in both the GW data and the EM data. However, around the time of detection of GW170817, the LIGO-Virgo detector network had a detection horizon of $\sim 190\,$Mpc for binary neutron star (BNS) events[1], within which EM measurements are largely complete. For example, the counterpart associated with GW170817 had brightness $\sim 17\,\mathrm{mag}$ in the I band at $40\,\mathrm{Mpc}$[28,30,31,52,53]; this source would be $\sim 22\,\mathrm{mag}$ at $400\,\mathrm{Mpc}$, and thus still detectable by survey telescopes such as DECam well beyond the GW horizon. Even the dimmest theoretical lightcurves for kilonovae are expected to peak at $\sim 22.5\,\mathrm{mag}$ at the LIGO–Virgo horizon[54]. We therefore expect that we are dominated by GW selection effects at the current time and can ignore EM selection effects. The fact that the fraction of BNS events that will have observed kilonova counterparts is presently unknown does not modify these conclusions, since we can restrict our analysis to GW events with kilonova counterparts only.

In the GW data, the decision about whether or not to analyse an event is largely determined by the signal-to-noise ratio (SNR), ρ, of the event. A reasonable model for the selection process is a cut in SNR, i.e., events with $\rho > \rho_*$ are analysed[55]. In that model, the integral over x_{GW} in Eq. (8) can be replaced by an integral over SNR from ρ_* to ∞, and $p(x_{\mathrm{GW}}|d, \cos\iota, \vec{\lambda})$ replaced by $p(\rho|d, \cos\iota, \vec{\lambda})$ in the integrand. This distribution depends on the noise properties of the operating detectors, and on the intrinsic strain amplitude of the source. The former are clearly independent of the population parameters, while the latter scales like a function of the source parameters divided by the luminosity distance. The dependence on source parameters is on redshifted parameters, which introduces an explicit redshift dependence. However, within the $\sim 190\,\mathrm{Mpc}$ horizon, redshift corrections are at most $\lesssim 5\%$, and the Hubble constant measurement is a weak function of these, meaning the overall impact is even smaller. At present, whether or not a particular event in the population ends up being analysed can therefore be regarded as a function of d only. When GW selection effects dominate, only the terms in Eq. (8) arising from the GW measurement matter. As these are a function of d only and we set a prior on d, there is no explicit H_0 dependence in these terms. Hence, $\mathcal{N}_\mathrm{s}(H_0)$ is a constant and can be ignored. This would not be the case if we set a prior on the redshifts of potential sources instead of their distances, since then changes in H_0 would modify the range of detectable redshifts. As the LIGO–Virgo detectors improve in sensitivity the redshift dependence in the GW selection effects will become more important, as will EM selection effects. However, at that point we will also have to consider deviations in the cosmological model from the simple Hubble flow described in Eq. (1) of the main article.

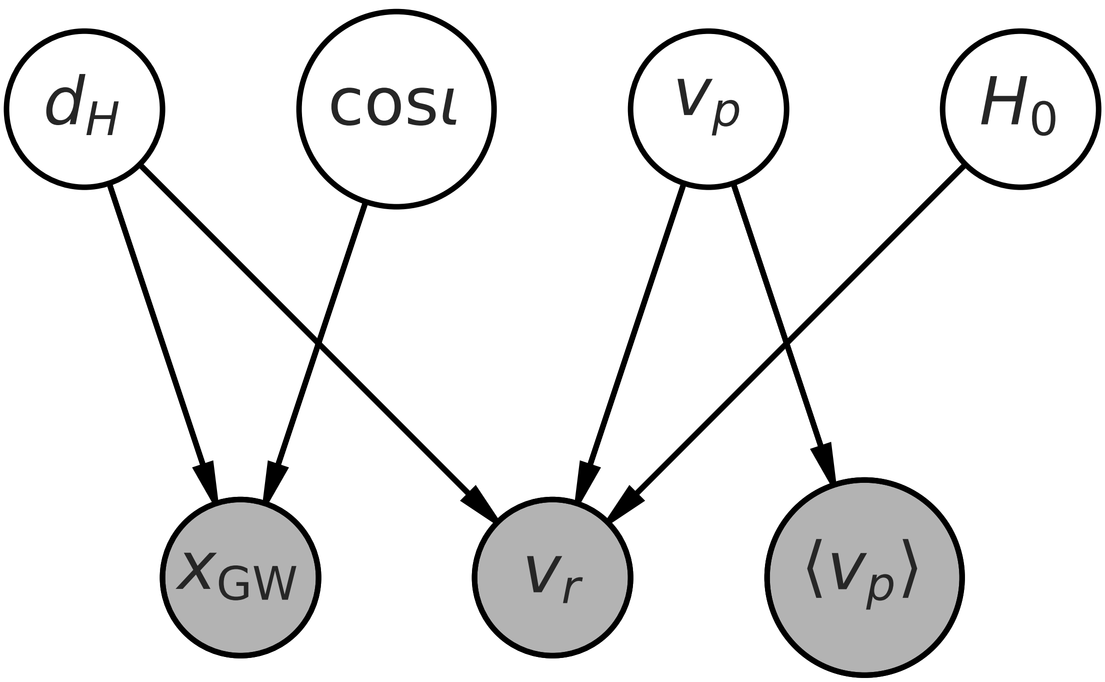

Extended Data Figure 1 A graphical model for our measurement, illustrating the mutual statistical relationships between the data and parameters in the problem. Open circles indicate parameters which require a prior; filled circles described measured data, which are conditioned on in the analysis. Here we assume we have measurements of the

GW data, x_{GW}, a recessional velocity (i.e. redshift), v_r, and the mean peculiar velocity in the neighborhood of NGC 4993, $\langle v_p \rangle$. Arrows flowing into a node indicate that the conditional probability density for the node depends on the source parameters; for example, the conditional distribution for the observed GW data, $p\,(x_{\mathrm{GW}} \mid d, \cos\iota)$, discussed in the text, depends on the distance and inclination of the source (and additional parameters, here marginalized out).

Marginalising Eq. (7) over d, v_p and $\cos\iota$ then yields

$$p(H_0 \mid x_{\mathrm{GW}}, v_r, \langle v_p \rangle) \propto p(H_0) \int p(x_{\mathrm{GW}} \mid d, \cos\iota)\, p(v_r \mid d, v_p, H_0)\, p(\langle v_p \rangle \mid v_p) \times\ p(d)\, p(v_p)\, p(\cos\iota)\, \mathrm{d}d\, \mathrm{d}v_p\, \mathrm{d}\cos\iota. \tag{9}$$

The posterior computed in this way was shown in Figure 1 in the main article and has a maximum a posteriori value and minimal 68.3% credible interval of $70^{+12}_{-8}\,\mathrm{km\,s^{-1}\,Mpc^{-1}}$, as quoted in the main article. The posterior mean is $78\,\mathrm{km\,s^{-1}\,Mpc^{-1}}$ and the standard deviation is $15\,\mathrm{km\,s^{-1}\,Mpc^{-1}}$. Various other summary statistics are given in Table 1.

Robustness to prior specification Our canonical analysis uses a uniform volumetric prior on distance, $p(d) \propto d^2$. The distribution of galaxies is not completely uniform due to clustering, so we explore sensitivity to this prior choice. We are free to place priors on any two of the three variables (d, H_0, z), where $z = H_0 d/c$ is the Hubble flow redshift of NGC 4993. A choice of prior for two of these variables induces a prior on the third which may or may not correspond to a natural choice for that parameter. A prior on z could be obtained from galaxy catalog observations, but must be corrected for incompleteness. When setting a prior on H_0 and z, the posterior becomes

$$p(H_0, z, \cos\iota, v_p \mid x_{\rm GW}, v_r, \langle v_p \rangle) \propto \frac{p(H_0)}{\mathcal{N}_{\rm s}(H_0)}\, p(x_{\rm GW} \mid d = cz/H_0, \cos\iota)\, p(v_r \mid z, v_p) \times\; p(\langle v_p \rangle \mid v_p)\, p(z)\, p(v_p)\, p(\cos\iota), \tag{10}$$

but now

$$\mathcal{N}_{\rm s}(H_0) = \int_{\rm detectable} p(x_{\rm GW} \mid d = cz/H_0, \cos\iota)\, p(v_r \mid z, v_p) \times\; p(\langle v_p \rangle \mid v_p)\, p(z)\, p(v_p)\, p(\cos\iota)\, {\rm d}z\, {\rm d}v_p\, {\rm d}\!\cos\iota\, {\rm d}x_{GW}\, {\rm d}v_r\, {\rm d}\langle v_p \rangle. \tag{11}$$

When GW selection effects dominate, the integral is effectively

$$\begin{aligned} p_{\rm det}(H_0) &= \int p(x_{\rm GW} \mid d = cz/H_0, \cos\iota) p(z)\, p(\cos\iota)\, {\rm d}z\, {\rm d}\!\cos\iota\, {\rm d}x_{GW} \\ &= \int p(x_{\rm GW} \mid d, \cos\iota) p(dH_0/c)\, p(\cos\iota)\, (H_0/c)\, {\rm d}d\, {\rm d}\!\cos\iota\, {\rm d}x_{GW}, \end{aligned} \tag{12}$$

which has an H_0 dependence, unless $p(z)$ takes a special, H_0-dependent form, $p(z) = f(z/H_0)/H_0$. However, if the redshift prior is volumetric, $p(z) \propto z^2$, the selection effect term is $\propto H_0^3$, which cancels a similar correction to the likelihood and gives a posterior on H_0 that is identical to the canonical analysis.

For a single event, any choice of prior can be mapped to our canonical analysis with a different prior on H_0. For any reasonable prior choices on d or z, we would expect to gradually lose sensitivity to the particular prior choice as further observed events are added to the analysis. However, to illustrate the uncertainty that comes from the prior choice for this first event, we compare in Figure 2 and Table 1 the results from the canonical prior choice $p\,(d) \propto d^2$ to those from two other choices: using a flat prior on z, and assuming a velocity correction due to the peculiar velocity of NGC 4993 that is a Gaussian with width $250\,\mathrm{km\,s^{-1}}$. (To do this analysis, the posterior samples from GW parameter estimation have to be re-weighted, since they are generated with the d^2 prior used in the canonical analysis. We first "undo" the default prior before applying the desired new prior.)

The choice of a flat prior on z is motivated by the simple model described above, in which we imagine first making a redshift measurement for the host and then use that as a prior for analysing the GW data. Setting priors on distance and redshift, the simple analysis gives the same result as the canonical analysis, but now we set a prior on redshift and H_0 and obtain a different result. This is to be expected because we are making different assumptions about the underlying population, and it arises for similar reasons as the different biases in peculiar velocity measurements based on redshift-selected or distance-selected samples[56]. As can be seen in Table 1, the results change by less than 1σ, as measured by the statistical error of the canonical analysis.

By increasing the uncertainty in the peculiar velocity prior, we test the assumptions in our canonical analysis that (1) NGC 4993 is a member of the nearby group of galaxies, and (2) that this group has a center-of-mass velocity close to the Hubble flow. The results in Table 1 show that there are only marginal changes in the values of H_0 or of the error bars.

We conclude that the impact of a reasonable change to the prior is small relative to the statistical uncertainties for this event.

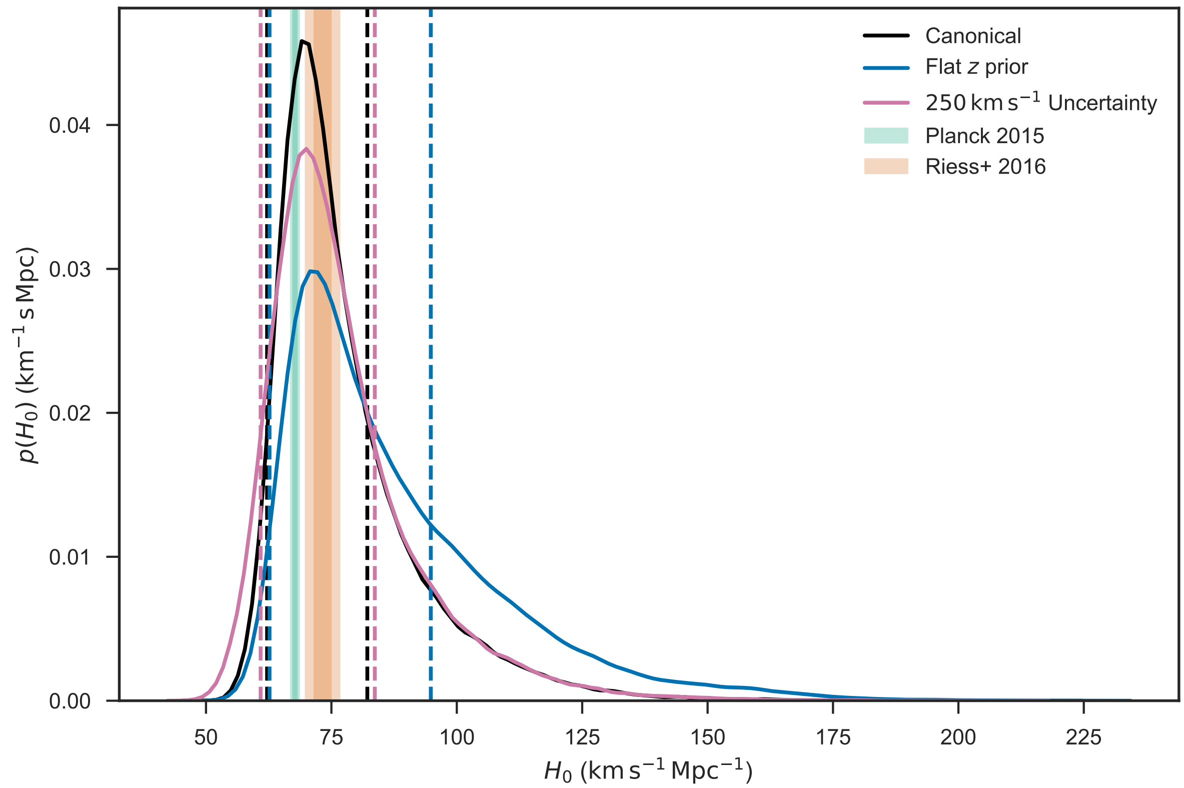

Extended Data Figure 2 Using different assumptions compared to our canonical analysis. The posterior distribution on H_0 discussed in the main text is shown in black, the alternative flat prior on z (discussed in the Methods section) gives the distribution shown in blue, and the increased uncertainty ($250\,\mathrm{km\,s^{-1}}$) applied to our peculiar velocity measurement (also discussed in the Methods section) is shown in pink. Minimal 68.3% (1σ) credible intervals are shown by dashed lines.

Incorporating additional constraints on H_0

By including previous measurements of H_0[38,39] we can constrain the orbital inclination more precisely. We do this by setting the H_0 prior in Eq. (7) to $p(H_0|\mu_{H_0}, \sigma^2_{H_0}) = N[\mu_{H_0}, \sigma^2_{H_0}]$, where

Table 1. Constraints on H_0 and $\cos\iota$ at varying levels of credibility. We give both one-sigma (68.3%) and 90% credible intervals for each quantity. "Symm." refers to a symmetric interval (e.g. median and 5% to 95% range), while "MAP" refers to maximum a posteriori intervals (e.g. MAP value and smallest range enclosing 90% of the posterior). Values given for ι are derived from arc-cosine transforming the corresponding values for $\cos\iota$, so the "MAP" values differ from those that would be derived from the posterior on ι.

Par.	68.3% Symm.	68.3% MAP	90% Symm.	90% MAP
$H_0/\left(\mathrm{km\,s^{-1}\,Mpc^{-1}}\right)$	74^{+16}_{-8}	70^{+12}_{-8}	74^{+33}_{-12}	70^{+28}_{-11}
$H_0/\left(\mathrm{km\,s^{-1}\,Mpc^{-1}}\right)$ (flat in z prior)	81^{+27}_{-13}	71^{+23}_{-9}	81^{+50}_{-17}	71^{+48}_{-11}
$H_0/\left(\mathrm{km\,s^{-1}\,Mpc^{-1}}\right)$ ($250\,\mathrm{km\,s^{-1}}$ σ_{v_r})	74^{+16}_{-9}	70^{+14}_{-9}	74^{+33}_{-14}	70^{+29}_{-14}
$\cos\iota$ (GW only)	$-0.88^{+0.18}_{-0.09}$	$-0.974^{+0.164}_{-0.026}$	$-0.88^{+0.32}_{-0.11}$	$-0.974^{+0.332}_{-0.026}$
$\cos\iota$ (SHoES)	$-0.901^{+0.065}_{-0.057}$	$-0.912^{+0.061}_{-0.059}$	$-0.901^{+0.106}_{-0.083}$	$-0.912^{+0.095}_{-0.086}$
$\cos\iota$ (Planck)	$-0.948^{+0.052}_{-0.036}$	$-0.982^{+0.06}_{-0.016}$	$-0.948^{+0.091}_{-0.046}$	$-0.982^{+0.104}_{-0.018}$
ι/deg (GW only)	152^{+14}_{-17}	167^{+13}_{-23}	152^{+20}_{-27}	167^{+13}_{-37}
ι/deg (SHoES)	154^{+9}_{-8}	156^{+10}_{-7}	154^{+15}_{-12}	156^{+21}_{-11}
ι/deg (Planck)	161^{+8}_{-8}	169^{+8}_{-12}	161^{+12}_{-12}	169^{+11}_{-18}
$d/\,(\mathrm{Mpc})$	$41.1^{+4}_{-7.3}$	$43.8^{+2.9}_{-6.9}$	$41.1^{+5.6}_{-12.6}$	$43.8^{+5.6}_{-13.1}$

for ShoES[39] $\mu_{H_0} = 73.24\,\mathrm{km\,s^{-1}\,Mpc^{-1}}$ and $\sigma_{H_0} = 1.74\,\mathrm{km\,s^{-1}\,Mpc^{-1}}$, while for Planck[38] $\mu_{H_0} = 67.74\,\mathrm{km\,s^{-1}\,Mpc^{-1}}$ and $\sigma_{H_0} = 0.46\,\mathrm{km\,s^{-1}\,Mpc^{-1}}$. The posterior on $\cos\iota$ is then

$$p(\cos\iota \mid x_{\mathrm{GW}}, v_r, \langle v_p\rangle, \mu_{H_0}, \sigma^2_{H_0}) \propto \int p(x_{\mathrm{GW}} \mid d, \cos\iota)\, p(v_r \mid d, v_p, H_0)\, p(\langle v_p\rangle \mid v_p) \times\, p(H_0|\mu_{H_0}, \sigma^2_{H_0})\, p(d)\, p(v_p)\, \mathrm{d}d\, \mathrm{d}v_p\, \mathrm{d}H_0. \quad (13)$$

This posterior was shown in Figure 3 of the main article.

1. Abbott *et al.* Gw170817: Observation of gravitational waves from a binary neutron star inspiral. Phys. Rev. Lett. **TBD** (2017). `TBD`.

2. LIGO Scientific Collaboration *et al.* Advanced LIGO. *Classical and Quantum Gravity* **32**, 074001 (2015). `1411.4547`.

3. Acernese, F. *et al.* Advanced Virgo: a second-generation interferometric gravitational wave detector. *Classical and Quantum Gravity* **32**, 024001 (2015). `1408.3978`.

4. Meegan, C. *et al.* The Fermi Gamma-ray Burst Monitor. ApJ **702**, 791–804 (2009). `0908.0450`.

5. Connaughton, V. *et al.* Ligo/virgo g298048: Fermi gbm trigger 170817.529 and ligo single ifo trigger. *GCN* **21506**, 1–+ (2017).

6. Savchenko, V. *et al.* Ligo/virgo g298048: Integral detection of a prompt gamma-ray counterpart. *GCN* **21507**, 1–+ (2017).

7. Goldstein, A. *et al.* Ligo/virgo g298048 - update on fermi/gbm grb 170817a analysis. *GCN* **21528**, 1–+ (2017).

8. Abbott *et al.* Gw170817 mma. Phys. Rev. Lett. **TBD** (2017). TBD.

9. Schutz, B. F. Determining the Hubble constant from gravitational wave observations. Nature **323**, 310–+ (1986).

10. Holz, D. E. & Hughes, S. A. Using gravitational-wave standard sirens. *The Astrophysical Journal* **629**, 15 (2005). URL http://stacks.iop.org/0004-637X/629/i=1/a=15.

11. Dalal, N., Holz, D. E., Hughes, S. A. & Jain, B. Short GRB and binary black hole standard sirens as a probe of dark energy. Phys. Rev. D **74**, 063006 (2006). astro-ph/0601275.

12. Nissanke, S., Holz, D. E., Hughes, S. A., Dalal, N. & Sievers, J. L. Exploring Short Gamma-ray Bursts as Gravitational-wave Standard Sirens. ApJ **725**, 496–514 (2010). 0904.1017.

13. Nissanke, S. *et al.* Determining the Hubble constant from gravitational wave observations of merging compact binaries. *ArXiv e-prints* (2013). 1307.2638.

14. Freedman, W. L. *et al.* Final Results from the Hubble Space Telescope Key Project to Measure the Hubble Constant. ApJ **553**, 47–72 (2001). astro-ph/0012376.

15. Del Pozzo, W. Inference of the cosmological parameters from gravitational waves: application to second generation interferometers. *Phys. Rev.* **D86**, 043011 (2012). 1108.1317.

16. Dalya, G., Frei, Z., Galgoczi, G., Raffai, P. & de Souza, R. S. VizieR Online Data Catalog: GLADE catalog (Dalya+, 2016). *VizieR Online Data Catalog* **7275** (2016).

17. Messenger, C. & Veitch, J. Avoiding selection bias in gravitational wave astronomy. *New Journal of Physics* **15**, 053027 (2013). `1206.3461`.

18. Veitch, J. *et al.* Parameter estimation for compact binaries with ground-based gravitational-wave observations using the LALInference software library. Phys. Rev. D **91**, 042003 (2015). `1409.7215`.

19. Hannam, M. *et al.* Simple Model of Complete Precessing Black-Hole-Binary Gravitational Waveforms. *Physical Review Letters* **113**, 151101 (2014).

20. Coulter, D. A. *et al.* Ligo/virgo g298048: Potential optical counterpart discovered by swope telescope. *GCN* **21529**, 1–+ (2017).

21. Cornish, N. J. & Littenberg, T. B. Bayeswave: Bayesian inference for gravitational wave bursts and instrument glitches. *Classical and Quantum Gravity* **32**, 135012 (2015). `1410.3835`.

22. Buonanno, A. & Damour, T. Effective one-body approach to general relativistic two-body dynamics. *Phys. Rev.* **D59**, 084006 (1999). `gr-qc/9811091`.

23. Blanchet, L. Gravitational Radiation from Post-Newtonian Sources and Inspiralling Compact Binaries. *Living Rev. Rel.* **17**, 2 (2014). `1310.1528`.

24. Hinderer, T. & Flanagan, É. É. Two-timescale analysis of extreme mass ratio inspirals in Kerr spacetime: Orbital motion. Phys. Rev. D **78**, 064028 (2008). `0805.3337`.

25. Vines, J., Flanagan, É. É. & Hinderer, T. Post-1-Newtonian tidal effects in the gravitational waveform from binary inspirals. Phys. Rev. D **83**, 084051 (2011). 1101.1673.

26. Sakai, S. *et al.* The Hubble Space Telescope Key Project on the Extragalactic Distance Scale. XXIV. The Calibration of Tully-Fisher Relations and the Value of the Hubble Constant. ApJ **529**, 698–722 (2000). astro-ph/9909269.

27. Abbott, B. P. *et al.* Properties of the Binary Black Hole Merger GW150914. *Phys. Rev. Lett.* **116**, 241102 (2016). 1602.03840.

28. Valenti, S. Ligo/virgo g298048: Dlt40 optical candidate. *GCN* **21531**, 1–+ (2017).

29. Arcavi, I. *et al.* Ligo/virgo g298048: Las cumbres observatory detection of the possible optical counterpart in ngc 4993. *GCN* **21538**, 1–+ (2017).

30. Tanvir, N. R. *et al.* Ligo/virgo g298048: Vista/vircam detection of candidate counterpart. *GCN* **21544**, 1–+ (2017).

31. Lipunov, V. *et al.* Ligo/virgo g298048: Master observations of the ngc 4993. *GCN* **21546**, 1–+ (2017).

32. Foley, R. J. *et al.* Ligo/virgo g298048: Inspection of archival hst data at the position of the potential optical counterpart. *GCN* **21536**, 1–+ (2017).

33. Hinshaw, G. *et al.* Five-Year Wilkinson Microwave Anisotropy Probe Observations: Data Processing, Sky Maps, and Basic Results. ApJS **180**, 225–245 (2009). 0803.0732.

34. Crook, A. C. *et al.* Groups of Galaxies in the Two Micron All Sky Redshift Survey. ApJ **655**, 790–813 (2007). astro-ph/0610732.

35. Crook, A. C. *et al.* Erratum: "Groups of Galaxies in the Two Micron All Sky Redshift Survey" (ApJ, 655, 790 [2007]). ApJ **685**, 1320–1323 (2008).

36. Springob, C. M. *et al.* The 6dF Galaxy Survey: peculiar velocity field and cosmography. MNRAS **445**, 2677–2697 (2014). 1409.6161.

37. Carrick, J., Turnbull, S. J., Lavaux, G. & Hudson, M. J. Cosmological parameters from the comparison of peculiar velocities with predictions from the 2M++ density field. MNRAS **450**, 317–332 (2015). 1504.04627.

38. Planck Collaboration *et al.* Planck 2015 results. XIII. Cosmological parameters. A&A **594**, A13 (2016). 1502.01589.

39. Riess, A. G. *et al.* A 2.4% Determination of the Local Value of the Hubble Constant. ApJ **826**, 56 (2016). 1604.01424.

40. Aubourg, É. *et al.* Cosmological implications of baryon acoustic oscillation measurements. Phys. Rev. D **92**, 123516 (2015). 1411.1074.

41. Bonvin, V. *et al.* H0LiCOW - V. New COSMOGRAIL time delays of HE 0435-1223: H_0 to 3.8 per cent precision from strong lensing in a flat ΛCDM model. MNRAS **465**, 4914–4930 (2017). 1607.01790.

42. Henning, J. W. *et al.* Measurements of the Temperature and E-Mode Polarization of the CMB from 500 Square Degrees of SPTpol Data. *ArXiv e-prints* (2017). 1707.09353.

43. Abbott, B. P. *et al.* Binary Black Hole Mergers in the First Advanced LIGO Observing Run. *Physical Review X* **6**, 041015 (2016). 1606.04856.

44. Abbott *et al.* Gw170814 : A three-detector observation of gravitational waves from a binary black hole coalescence. Phys. Rev. Lett. **TBD** (2017). TBD.

45. Huang, J.-S., Cowie, L. L. & Luppino, G. A. Morphological Classification of the Local I- and K-Band Galaxy Sample. ApJ **496**, 31–38 (1998).

46. Bloom, J. S., Kulkarni, S. R. & Djorgovski, S. G. The Observed Offset Distribution of Gamma-Ray Bursts from Their Host Galaxies: A Robust Clue to the Nature of the Progenitors. AJ **123**, 1111–1148 (2002). astro-ph/0010176.

47. Skrutskie, M. F. *et al.* The Two Micron All Sky Survey (2MASS). AJ **131**, 1163–1183 (2006).

48. Jones, D. H. *et al.* The 6dF Galaxy Survey: final redshift release (DR3) and southern large-scale structures. MNRAS **399**, 683–698 (2009). 0903.5451.

49. Huchra, J. P. *et al.* The 2MASS Redshift Survey—Description and Data Release. ApJS **199**, 26 (2012). 1108.0669.

50. Loredo, T. J. Accounting for Source Uncertainties in Analyses of Astronomical Survey Data. In Fischer, R., Preuss, R. & Toussaint, U. V. (eds.) *American Institute of Physics Confer-*

ence Series, vol. 735 of *American Institute of Physics Conference Series*, 195–206 (2004). astro-ph/0409387.

51. Mandel, I., Farr, W. M. & Gair, J. Extracting distribution parameters from multiple uncertain observations with selection biases. Tech. Rep., LIGO (2016). https://dcc.ligo.org/LIGO-P1600187/public.

52. Arcavi, I. *et al.* Ligo/virgo g298048: Galaxy-targeted optical followup with las cumbres observatory. *GCN* **21543**, 1–+ (2017).

53. Coulter, D. A. *et al.* Ligo/virgo g298048: Correction to swope photometry announced in lvc gcn 21529. *GCN* **21567**, 1–+ (2017).

54. Metzger, B. D. & Berger, E. What is the Most Promising Electromagnetic Counterpart of a Neutron Star Binary Merger? ApJ **746**, 48 (2012). 1108.6056.

55. Abbott, B. P. *et al.* Supplement: "The Rate of Binary Black Hole Mergers Inferred from Advanced LIGO Observations Surrounding GW150914" (2016, ApJL, 833, L1). ApJS **227**, 14 (2016). 1606.03939.

56. Strauss, M. A. & Willick, J. A. The density and peculiar velocity fields of nearby galaxies. Phys. Rep. **261**, 271–431 (1995). astro-ph/9502079.

Acknowledgements The authors gratefully acknowledge the support of the United States National Science Foundation (NSF) for the construction and operation of the LIGO Laboratory and Advanced LIGO as well as the Science and Technology Facilities Council (STFC) of the United Kingdom, the Max-Planck-Society (MPS), and the State of Niedersachsen/Germany for support of the construction of Advanced LIGO and construction and operation of the GEO600 detector. Additional support for Advanced LIGO was provided by the Australian Research Council. The authors gratefully acknowledge the Italian Istituto Nazionale di Fisica Nucleare (INFN), the French Centre National de la Recherche Scientifique (CNRS) and the Foundation for Fundamental Research on Matter supported by the Netherlands Organisation for Scientific Research, for the construction and operation of the Virgo detector and the creation and support of the EGO consortium. The authors also gratefully acknowledge research support from these agencies as well as by the Council of Scientific and Industrial Research of India, the Department of Science and Technology, India, the Science & Engineering Research Board (SERB), India, the Ministry of Human Resource Development, India, the Spanish Agencia Estatal de Investigación, the Vicepresidència i Conselleria d'Innovació, Recerca i Turisme and the Conselleria d'Educació i Universitat del Govern de les Illes Balears, the Conselleria d'Educació, Investigació, Cultura i Esport de la Generalitat Valenciana, the National Science Centre of Poland, the Swiss National Science Foundation (SNSF), the Russian Foundation for Basic Research, the Russian Science Foundation, the European Commission, the European Regional Development Funds (ERDF), the Royal Society, the Scottish Funding Council, the Scottish Universities Physics Alliance, the Hungarian Scientific Research Fund (OTKA), the Lyon Institute of Origins (LIO), the National Research, Development and Innovation Office Hungary (NKFI), the National Research Foundation of Korea, Industry Canada and the Province of Ontario through the Ministry of Economic Development and Innovation, the Natural Science and Engineering Research Council Canada, the Canadian Institute for Advanced Research, the Brazilian Ministry of Science, Technology, Innovations, and Communications, the International Center for Theoretical Physics South American Institute for Fundamental Research (ICTP-SAIFR), the Research Grants Council of Hong Kong, the National Natural Science Foundation of China (NSFC), the Leverhulme

Trust, the Research Corporation, the Ministry of Science and Technology (MOST), Taiwan and the Kavli Foundation. The authors gratefully acknowledge the support of the NSF, STFC, MPS, INFN, CNRS and the State of Niedersachsen/Germany for provision of computational resources. This article has been assigned the document number LIGO-P1700296.

Competing Interests The authors declare that they have no competing financial interests.

Correspondence Correspondence and requests for materials should be addressed to A.B.C. (email: myaddress@nowhere.edu).